

OPEN ACCESS

Simulation studies to optimize the process of plasma spray deposition of yttrium oxide

To cite this article: T K Thiyagarajan *et al* 2010 *J. Phys.: Conf. Ser.* **208** 012116

View the [article online](#) for updates and enhancements.

Related content

- [Modelling of non-transferred argon-nitrogen plasma arc and plasma jet](#)
B Selvan, K Ramachandran, T K Thiyagarajan *et al.*
- [Numerical modelling of plasma spray process](#)
K Ramachandran
- [Effects of plasma parameters and collection region on synthesis of iron and nickel aluminide composite particles during thermal plasma processing](#)
K Suresh and V Selvarajan

Recent citations

- [Macroscopic Modeling of an Agglomerated and Sintered Particle in Air Plasma Spraying](#)
K. Bobzin *et al*
- [Macroscopic particle modeling in air plasma spraying](#)
K. Bobzin *et al*
- [Modeling Plasma-Particle Interaction in Multi-Arc Plasma Spraying](#)
K. Bobzin and M. Öte



ECS **240th ECS Meeting**
Oct 10-14, 2021, Orlando, Florida

Register early and save up to 20% on registration costs

Early registration deadline Sep 13

REGISTER NOW

Simulation studies to optimize the process of plasma spray deposition of yttrium oxide

T K Thiyagarajan¹, K P Sreekumar¹, V Selvan²,
K Ramachandran² and P V Ananthpadmanabhan²

¹Laser and Plasma Technology Division
Bhabha Atomic Research Centre, Trombay, Mumbai 400 085, India

²School of Mechanical and Building Sciences,
Vellore Institute of Technology, Vellore-632014, India

Abstract. Simulation studies on the thermal behaviour of yttrium oxide particles in a thermal plasma jet was carried out with the objective of controlling and optimization of the plasma spray process. The 'in-flight' behaviour of yttrium oxide particles in the plasma jet was studied by solving the heat transfer and momentum transfer equations using the velocity and temperature distribution in the plasma jet obtained from a two-dimensional model. In particular, the effect of particle size, thermal power of the torch and the torch operating parameters like gas flow rates were considered to calculate the heat transfer and momentum transfer to the particle. Results of simulation studies agree quite well with the experimental results on variation of deposition efficiency with power and particle size. The complete description of the model with the results obtained for the typical operating parameters of our plasma spray torch is presented in the paper.

1. Introduction

Plasma spray processes have been widely used to produce various metallic and ceramic coatings for wear resistance, corrosion resistance and thermal protection due to its relative high flame temperature and in-flight heat transfer and momentum transfer to the injected powder particles. To maintain a quality control for the coating with desirable functionality, the control and optimization of this process has to be done based on the scientific understanding of the complex heat and momentum transfer involved between the particles and the hot fluid. Moreover to model these heat and momentum transfer phenomena in realistic situation, the temperature and the velocity distribution of the plasma all over the flow region is required. The modeling of plasma spray process has received considerable attention in order to get the velocity and temperature distribution in the fluid region using computational fluid dynamics. Also, the interaction between the in-flight particle and plasma jet is studied by various research workers.

To optimise the torch operating parameters and the particle size for the process of yttrium oxide coating, we predicted the yttrium oxide particle's velocity and temperature during the in-flight time by developing a axi-symmetric cylindrical two-dimensional model for the plasma flow specific to our plasma spray torch. The temperature and the velocity distribution obtained from this model for the plasma in the flow region is used to analyse the heat transfer and momentum transfer from the fluid to the particle during in-flight. By solving the respective equations for heat transfer and momentum

transfer, we are able to predict the trajectory and thermal state of the yttrium oxide particle of given size for various operating parameters of the plasma spray torch.

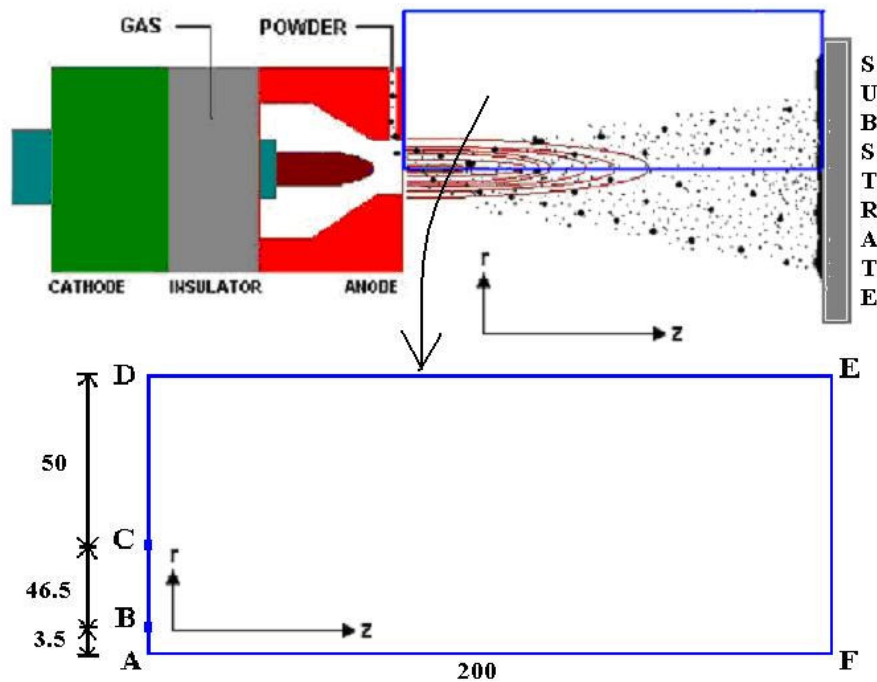


Figure 1. Schematic diagram of the process of spraying using Plasma spray torch. The computational domain is also shown for the Plasma jet modeling.

2. Plasma jet modeling

The schematic presentation of plasma spray process and computational geometry (the typical dimensions are given in mm) is displayed in figure 1. The Plasma jet is treated as a compressible and turbulent flow with temperature dependent thermodynamic and transport properties with the assumption of local thermodynamic equilibrium.

The mathematical formulation is based on the following assumptions.

- Flow is assumed two-dimensional. Temperature and flow fields are assumed to be axial symmetric. Two-dimensional cylindrical coordinates system($r - z$) is used.
- The plasma jet is treated as a compressible and turbulent flow with temperature dependent thermodynamic and transport properties
- Local thermodynamic equilibrium is assumed.

The following set of equations is used for modeling the plasma in the region ABCDEFA as shown in figure 1.

Conservation of mass:

$$\frac{\partial}{\partial z}(\rho u) + \frac{1}{r} \frac{\partial}{\partial r}(\rho r v) = 0 \quad (1)$$

Conservation of Axial momentum

$$\rho u \frac{\partial u}{\partial z} + \rho v \frac{\partial u}{\partial r} = -\frac{\partial p}{\partial z} + 2 \frac{\partial}{\partial z} \left(\mu \frac{\partial u}{\partial z} \right) + \frac{1}{r} \frac{\partial}{\partial r} \left(\mu r \frac{\partial u}{\partial r} \right) + \frac{1}{r} \frac{\partial}{\partial r} \left(\mu r \frac{\partial v}{\partial z} \right) \quad (2)$$

Conservation of Radial momentum

$$\rho u \frac{\partial v}{\partial z} + \rho v \frac{\partial v}{\partial r} = -\frac{\partial p}{\partial r} + \frac{\partial}{\partial z} \left(\mu \frac{\partial v}{\partial z} \right) + \frac{2}{r} \frac{\partial}{\partial r} \left(\mu r \frac{\partial v}{\partial r} \right) + \frac{\partial}{\partial z} \left(\mu \frac{\partial u}{\partial r} \right) - \frac{2\mu v}{r^2} \quad (3)$$

Conservation of Thermal Energy

$$\rho u \frac{\partial h}{\partial z} + \rho v \frac{\partial h}{\partial r} = \frac{\partial}{\partial z} \left(\frac{k}{C_p} \frac{\partial h}{\partial z} \right) + \frac{1}{r} \frac{\partial}{\partial r} \left(\frac{kr}{C_p} \frac{\partial h}{\partial r} \right) + -4\pi\epsilon_N \quad (4)$$

Where u and v are the axial and radial velocity components. P is the local pressure, h is the specific enthalpy, z and r are the distances in axial and radial directions respectively. ρ , μ , C_p , and κ are respectively the mass density, viscosity, specific heat and thermal conductivity of the plasma. ϵ_N is the net emission coefficient of the plasma which is used for calculating the radiation losses. The equations (1) to (4) are solved with proper boundary conditions using the SIMPLER algorithm. The boundary conditions are given in table 1. The temperature distribution and the fluid streamline obtained from the solution of these equations for a typical flow rate and power is shown in figure 2. After obtaining the temperature and velocity distribution in the plasma region, the temperature profile and the fluid axial velocity profile along the flow direction is plotted in the figure 3. For getting the temperature profile, the temperature is averaged along the radial direction at each axial grid location over the circular area of radius 3.5 mm. This circular area of radius 3.5 mm is equal to the nozzle area. These temperature and velocity profiles are used for solving the particle momentum transfer and particle heat transfer equations.

3. Mathematical Formulation Of Plasma-Particle Interaction.

A solid particle injected into the thermal plasma will usually undergo the following processes.

- Solid particle heating from initial temperature to melting point.
- Melting of the solid particle at a constant temperature till it is completely molten.
- Heating of molten solid

The following assumptions are made for the theoretical modeling.

- Heating of single Y_2O_3 particle is considered.
- The particle is exposed to Ar- N_2 Plasma.
- The particle vapour does not affect the thermo dynamical and thermo physical properties of Ar- N_2 Plasma.
- Radiation from and to the particle is neglected.

In thermal plasma spray, the velocity and the trajectory of an injected particle is mainly affected by the viscous drag, the governing equation for momentum transfer between single spherical particle of mass m_p and the plasma gas can be written as

$$m_p \frac{du_p}{dt} = \frac{1}{4} C_D \pi D_p^2 \left(\frac{1}{2} \rho_g |u_g - u_p|^2 \right) \quad (5)$$

Where u_p is the velocity of particle, C_D is the drag coefficient, D_p is the particle Diameter, ρ_g is the plasma density and u_g is the plasma velocity. Eqn. 5 can be written in simplified form in terms of particle's diameter and particles' Density as follows

$$\frac{du_p}{dt} = \frac{3 C_D \rho_g}{4 \rho_p d} |u_g - u_p|^2 \quad (6)$$

The initial condition given to solve the above eqn.(6) is $u_p = 0$ when $t=0$. The equation describing the heat balance between the particle and the flame is given by

$$\pi D_p^2 h (T_g - T_p) = \frac{1}{6} \pi \rho_p C_p D_p^3 \frac{dT_p}{dt} \quad (7)$$

Where h is the heat transfer coefficient. The left side of eqn.7 represents the rate of heat transferred to particle from plasma and the right side of eqn.7 represents the rate of heat absorbed by the particle. The heat transfer coefficient is obtained from the Nusselt Number which is described for spherical shape particle is

$$Nu = \frac{h D_p}{k} = 2 + 0.66 Re^{0.5} Pr^{0.33} \quad (8)$$

Where k is the thermal conductivity of the plasma, Re is the Reynold number and Pr is the Prantal Number. Eqn. 7 is solved with the initial condition $T_p =$ ambient temperature at $t=0$; To solve the eqns. 6 and 7 we use the velocity and temperature profiles for plasma which are obtained by solving fluid dynamic equations in the plasma region. The material properties of Y_2O_3 are given in the table 2. The Specific heat of Y_2O_3 as a function of temperature upto 1330K is shown in figure 2 and the specific heat remains constant after 1330 K. The tabulated values available for thermodynamic properties and transport properties of Ar-N₂ plasma is fitted into polynomial form in different temperature region and is used for solving the momentum transport and heat balance equation. The eqns. 6 and 7 are solved using Runga – Kutta method.

4. Results and Discussion

Calculations are done for the torch operating parameters listed in table 3. Torch operating power is varied from 20 kW to 30 kW in steps of 5 kW. The electro-thermal efficiency is assumed as 60%. The primary argon flow rates considered are 25 and 30 LPM. 12 LPM of powder carrier Ar flow rate is considered as secondary flow rate. Hence total argon flow rates were 37 LPM and 42 LPM. In addition to these primary and secondary Ar gas flow rates, 3 LPM of N₂ flow rate also considered. Powder feed rate is 10 g/min. The temperature and velocity of various particle sizes from 60 micron to 100 micron is plotted in the figure 5 for the torch input power 30kW. Table 4 shows the maximum temperature and velocity obtained for the particles of different sizes for various operating parameters of the torch.

Table 1. Boundary conditions used for solving Fluid dynamic equations .

| Boundary | Axial velocity V | Radial Velocity u | Enthalpy h |
|--|--|-----------------------------|---|
| AB Nozzle exit | Inlet velocity profile is specified using total mass flow rate | U = 0; | Inlet Temperature Profile is specified using energy balance |
| BC Torch wall | V = 0 | U = 0; | Wall Temperature is specified |
| CD Entrainment Region | Continuity Equation with U=0 | U =0 | Ambient Temperature |
| DE Extreme Boundary, r = 100 | V = 0 | Continuity eqn. With V = 0; | Ambient Temperature |
| EF Extreme Boundary, z = 200 | V=0; | U=0; | Ambient Temperature |
| AF (Axial boundary, line of Symmetry) | | Radial Gradient vanishes | |

Table 2. Physical Properties of Y_2O_3

| | |
|----------------------|------|
| Density (kg/m^3) | 5010 |
| Melting Point (K) | 2963 |
| Boiling Point (K) | 5010 |

Table 3. Operating Parameters of the torch used for the calculations

| Parameter | Range |
|--|---------|
| Torch input power (kW) | 20 - 30 |
| Plasma gas(Ar) flow rate (LPM) | 25 - 30 |
| Secondary gas(N_2) flow rate (LPM) | 3 |
| Powder feed rate (g/min) | 13 - 14 |
| Powder carrier gas flow rate (LPM) | 12 |

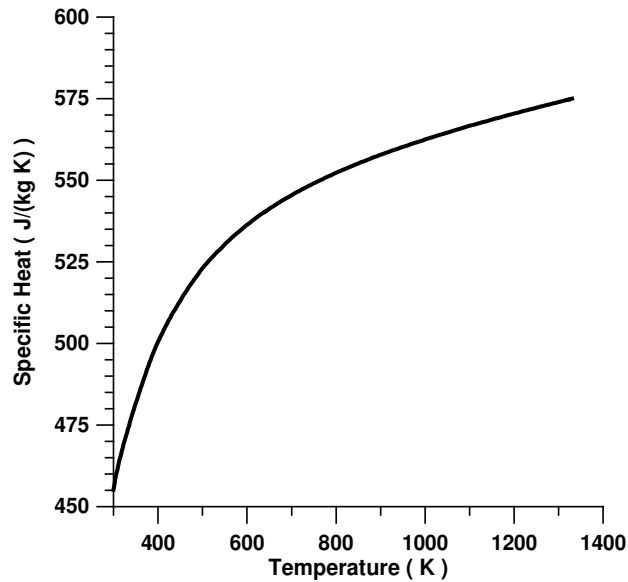


Figure 2. Specific heat of Y₂O₃ plotted as a function of temperature

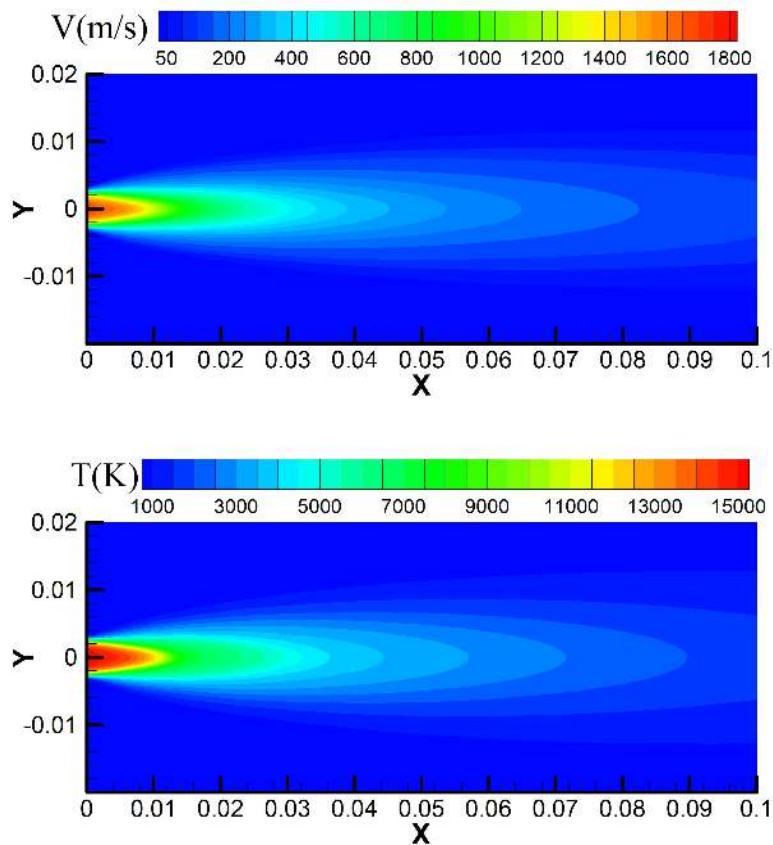


Figure 3. Temperature and velocity distribution obtained for plasma jet modeling for the torch input power 30 kW and Ar flow rate 42 LPM

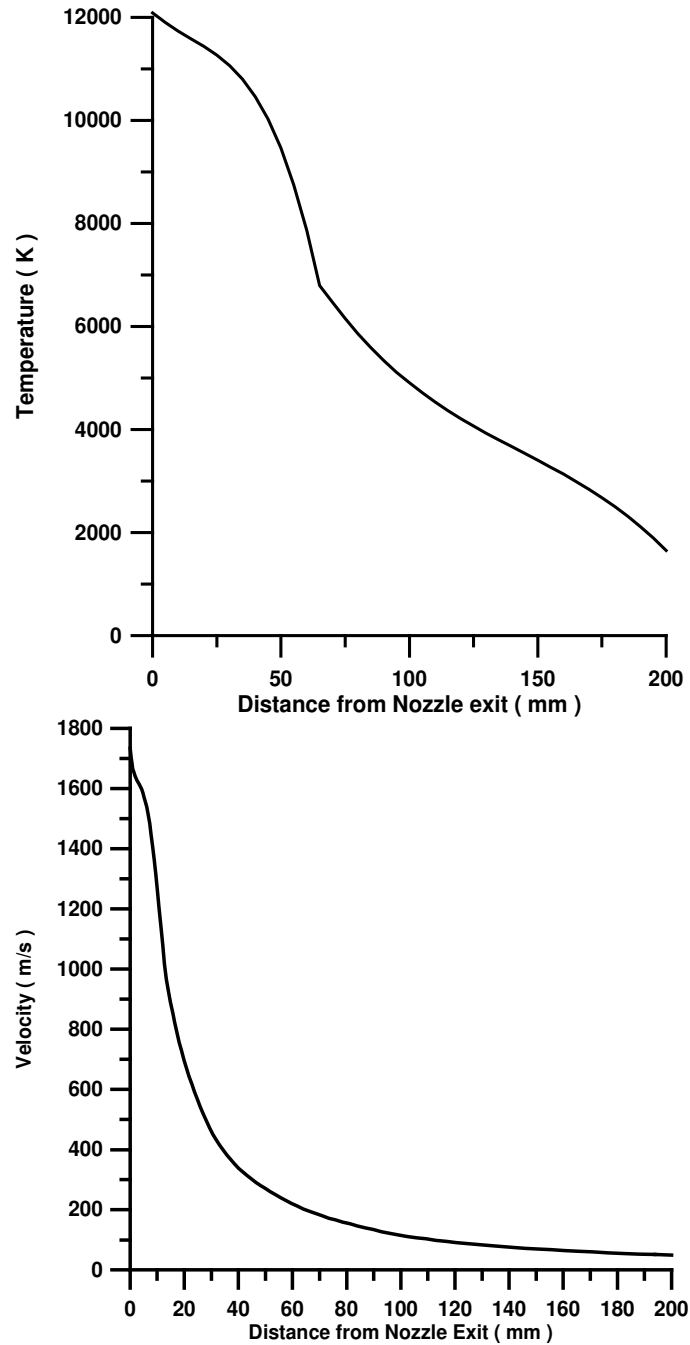


Figure 3. Velocity and Temperature of Plasma at Axial Line of the Spray Torch obtained by Solving Fluid Dynamic Equations

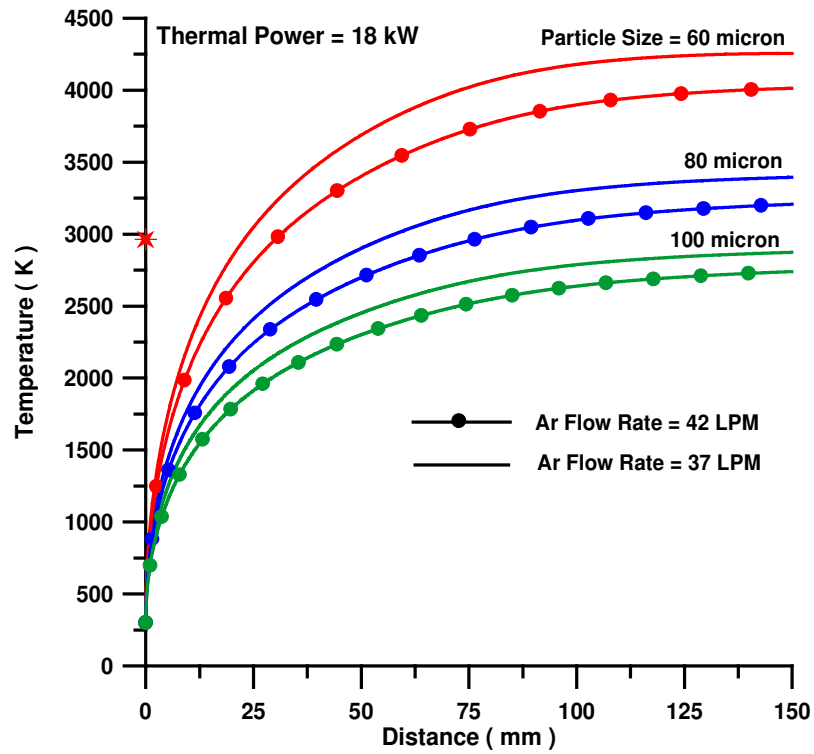
Table 4. Calculated values of maximum temperature and velocity for the various size Y_2O_3 particles and for the different torch operating parameters

| Ar Flow (LPM) | Power (kW) | Inlet Plasma Temperature(K) | Particle Size (μm) | Tmax (K) | Umax (m/s) |
|---------------|------------|-----------------------------|---------------------------------|-------------------|------------|
| 42 | 30 | 14800 | 60 | 3899 | 137 |
| | | | 80 | 3097 | 104 |
| | | | 100 | 2640 [#] | 100 |
| 42 | 25 | 14020 | 60 | 3504 | 133 |
| | | | 80 | 2804 [#] | 101 |
| | | | 100 | 2388 [#] | 97 |
| 42 | 20 | 13125 | 60 | 3056 | 121 |
| | | | 80 | 2502 [#] | 97 |
| | | | 100 | 2117 [#] | 82 |
| 37 | 30 | 15260 | 60 | 4179 | 125 |
| | | | 80 | 3303 | 101 |
| | | | 100 | 2788 [#] | 86 |
| 37 | 25 | 14450 | 60 | 3819 | 122 |
| | | | 80 | 3030 | 99 |
| | | | 100 | 2583 [#] | 82 |
| 37 | 20 | 13525 | 60 | 3483 | 113 |
| | | | 80 | 2806 [#] | 94 |
| | | | 100 | 2408 [#] | 77 |

N₂ Flow = 3 LPM, Electro Thermal Efficiency of torch = 0.6, * Boiling Point of Y_2O_3 = 4573 K
[#] Temperature below Melting point 2963 K

The calculated temperature profile of Y_2O_3 particles given in figure 4 and the results tabulated in table 4 clearly shows that the temperature attained by the particle strongly depends on the particle size and the input power. It is seen from the figure 4 that for a given set of plasma power and other operating conditions, the maximum temperature obtained by the particle varies inversely on the particle size. Also lower gas flow rate makes the particle of given size gives more particle's temperature in comparison with the higher flow rate. Results given in table 4 indicate that at 20kW input power with total gas flow rates of 37 LPM and 42 LPM, particle of 60-micron size attains the temperature above the melting point 2963 K. However particles of size 80-micron and 100-micron do not reach the melting point for the same torch input power level. 80-micron size particle do not reach melting point at 25kW and 42 LPM total gas flow rate. However when the total gas flow is reduced to 37 LPM, 25 kW is just sufficient to melt the particle of 80-micron size. Table 5 gives the experimental results obtained for adhesion strength of Y_2O_3 coating on SS substrate with the similar torch

operating parameters used in calculations. We can see that the results of adhesion strength reflect the inferences we get from the calculated results



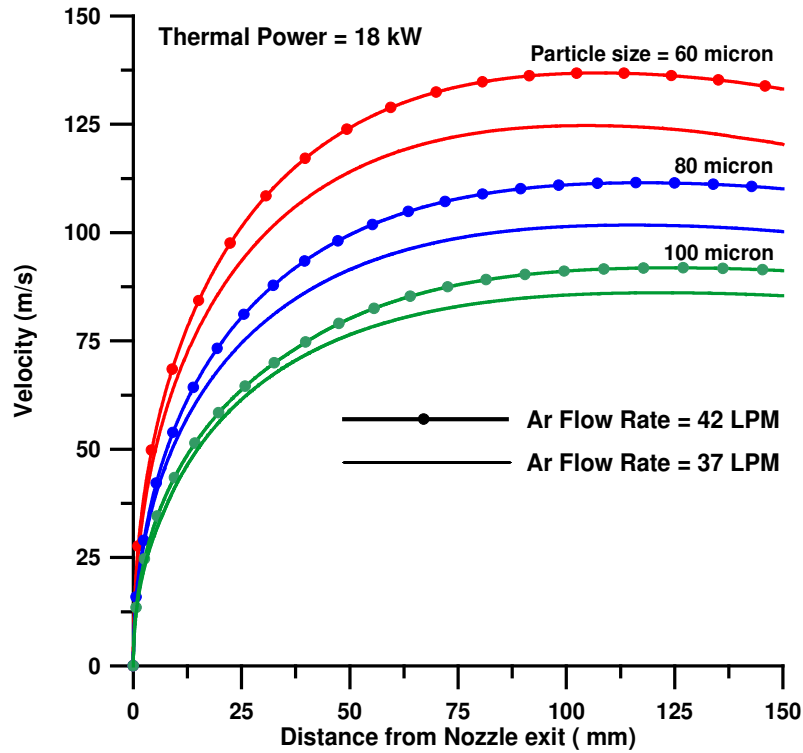


Figure 4. Calculated temperature and velocity of different size Y_2O_3 particles along the flow direction for the torch thermal power 18 kW and for Ar flow rates 42 and 37 LPM

Table 5. Experimental results for the Adhesion Strength of Y_2O_3 Powder sprayed on SS substrate

| Powder Size (μm) | Current (A) | Voltage (V) | Power (kW) | Primary Ar Gas (LPM) | Coating Thickness (μm) | Adhesion strength (Mpa) |
|-------------------------------|-------------|-------------|------------|----------------------|-------------------------------------|-------------------------|
| 38-75 | 700 | 42 | 29.4 | 30 | 250 | 7.276 |
| 38-75 | 680 | 44 | 29.9 | 25 | 250 | 5.238 |
| 38-75 | 560 | 44 | 24.6 | 30 | 250 | 4.178 |
| 38-75 | 580 | 42 | 24.4 | 25 | 250 | 4.892 |
| 76-106 | 680 | 44 | 29.9 | 30 | 280 | 8.051 |
| | | | | | | 7.032 |
| | | | | | | 6.013 |
| | | | | | | 6.053 |
| | | | | | | 5.605 |
| | | | | | | 6.053 |

| | | | | | | |
|--------|-----|----|------|----|-----|----------------|
| 76-106 | 680 | 44 | 29.9 | 25 | 280 | 4.280 3.322 |
| 76-106 | 580 | 44 | 24.6 | 30 | 280 | 4.994 5.911 |
| 76-106 | 580 | 44 | 24.6 | 25 | 280 | 4.076 3.689 |

| | |
|-----------------------------|------------------|
| Carrier gas (Ar) Flowrate | :- 12 LPM |
| Secondary Gas | :- 3 LPM |
| Powder feeding rate | :- 13 – 14 g/min |
| Torch to Substrate Distance | :- 100 mm |
| Substrate Material | :- SS |

5. Conclusion

Two-dimensional model for plasma jet specific to our plasma spray torch is developed to get the temperature and velocity distribution in the flow region. The temperature and velocity profile obtained from this two-dimensional model is used to predict the Y₂O₃ particle's velocity and the temperature during in-flight for the given size of particle and torch operating parameters like input power and total gas flow rates. The predicted temperature history and the trajectory are correlated with the experimental results of the Adhesion Strength of Y₂O₃ Powder sprayed on SS substrate.

6. References

- [1] Hong-Bing Xiong, Li-Li Zheng, Sanjay Sampath, Richard L. Williamson and Jim R. Fincke 2004 Three-dimensional simulation of plasma spray: effects of carrier gas flow and particle injection on plasma jet and entrained particle behaviour *Int. J. Heat and Mass Trans.* **47** 5189
- [2] J.D.Ramshaw, C.H.Chang Computational fluid dynamics modeling of multi-component thermal plasmas, 1992 *Plasma Chem. Plasma Process.* **12** 299-325
- [3] K. Ramachandran and H.Nishiyama, Three-dimensional effects of carrier gas and particle injection on the thermo-fluid fields of plasma jets 2002 *J.Phys. D: Appl.Phys.* **35** 307-317
- [4] K. Ramachandran and V.Selvarajan, Trajectory and temperature history of the particles of different sizes and their injection velocities in a thermal plasma 1996 *Comp. Mat. Sci.* **6** 81-91
- [5] P.V.Ananthapadmanabhan, T.K.Thiyagarajan, K.P.Sreekumar and N.Venkatramani 2004 Formation of nano-sized alumina by in-flight oxidation of aluminium powder in a thermal plasma reactor, *Scripta Mat.* **50** 143-147